

# Stress Field Expressions Useful to the Analysis of Crack Initiation and Early Propagation Phases in Notched Shafts Under Torsion

M. Zappalorto<sup>1</sup>, S. Filippi<sup>2</sup>, P. Lazzarin<sup>1</sup>

<sup>1</sup> University of Padova, Dept. Management and Engineering, , Stradella. S.Nicola 3, 36100 Vicenza (Italy).

<sup>2</sup> Omera, s.r.l. - Via Ponte Dei Granatieri, 8 - 36010 Chiuppano-VI (Italy)

zappalorto@gest.unipd.it, plazzarin@gest.unipd.it

**ABSTRACT.** *The present work is aimed at providing some expressions for stress distributions due to U- and V-shaped notches in rounded bars under torsion, including the finite size effect. By taking advantage of the global equilibrium conditions, the shear stress distributions are determined not only in the vicinity of the notch root but also on the entire net section of the shaft.*

*The degree of accuracy of the new closed form relationships is checked by a number of FE analyses carried out on finite size components subjected to torsion loads.*

## INTRODUCTION

In structural components fatigue cracks initiate and propagate from the highly stressed zones where notches provoke perturbations of the stress fields.

The knowledge of theoretical stress concentration factors and local stress distributions in the neighbourhood of the geometrical stress raisers is essential for engineers engaged in fatigue design and fatigue crack growth problems. Indeed, as the notch radius decreases, brittle failure as well as high cycle fatigue failure are no longer controlled by the peak stress value but rather by the stress fields present in the highly stressed zones. When the notch tip radius tends to zero, the magnitude of the stress distributions is often given in terms of stress intensity factors or notch stress intensity factors, the latter valid for V-notches with an opening angle different from zero. Taking advantage of Bueckner's superposition principle, not only the crack initiation phase but also the early crack propagation phase can be predicted in all cases on the basis of the stress distributions initially determined on the uncracked component.

In the previous literature notch problems have then been extensively analysed by taking advantage both of analytical approaches, see Refs [1-3] among the most important contributions, or numerical methods [4, 5]; these works mainly dealt with notches under tensile or bending loadings. On the contrary, even if the engineering use of torque carrying shafts is extensive, being them susceptible to crack formation at notches and

grooves, only few works were focused on torsional loading of prismatic shafts; among these contributions, the most important one is due to Neuber [6].

Some analytical solutions of the stress distributions in notched components under torsion have been recently reported in the literature [7, 8] taking into account semi-elliptical, parabolic or hyperbolic notches in round shafts.

When components can be considered as infinite, stress distributions are not influenced by external boundaries and depend only on the relevant boundary conditions provided by the notch shape; on the contrary as dimensions decrease the outer boundaries begin to exert a strong influence [8].

Complete and exact analytical solutions for finite bodies are not impossible, but typically involve a series-approximation-based approach that leads to results less manageable with respect to the co-respective infinite body-based treatise [9, 10]. Such an approach may be useful even when the notch profile cannot be described by means of a unique continuous function, such as in the case of a U-notch [11].

Differently from those important contributions, in this work we will discard the series-based approach, and provide simple but accurate expressions for the stress fields due to U- and V-rounded notches under torsion by starting from the analytical solution valid for hyperbolic and parabolic notches. The finite size effect will also be considered by taking advantage of a global equilibrium condition, as suggested in Refs. [12-14] dealing with components under tension loads. In such a way the expressions for shear stresses will be accurate not only in the vicinity of the notch root but also on the entire net section of the shaft. The accuracy of the new closed-form relationships is checked by a number of FE analyses carried out on finite size components subjected to torsion loads.

## HYPERBOLIC AND PARABOLIC NOTCHES UNDER TORSION

Stress distributions for hyperbolic and parabolic notches under torsion loading have been recently provided by Zappalorto *et al.* [8] by using, in combination, Neuber's curvilinear coordinate system [6] and a complex potential approach linking shear stresses to a unic holomorphic function,  $\tau_{zr} - i \tau_{z\varphi} = e^{i\varphi} z^{\lambda-1}$ .

By imposing appropriate boundary conditions, stresses were written as functions of the maximum shear stress at the notch tip according to the following expression (see also figure 1) [8]:

$$\begin{cases} \tau_{zr}(r,\varphi) \\ \tau_{z\varphi}(r,\varphi) \end{cases} = \tau_{\max} \left( \frac{r}{r_0} \right)^{\lambda_3-1} \begin{cases} \sin \lambda_3 \varphi \\ \cos \lambda_3 \varphi \end{cases} \left( 1 - \frac{(r-r') \cos \varphi}{R'} \right) \quad (1a-b)$$

The geometrical parameters  $q$ ,  $r_0$ ,  $r'$  are given as follows [8]:

$$q = \frac{2\pi - 2\alpha}{\pi} = \frac{1}{\lambda_3} \quad r_0 = \frac{q-1}{q} \rho \quad r' = \frac{r_0}{(\cos(\varphi/q))^q} \quad (2)$$

Along the notch bisector line Eqs. (1b) simplifies:

$$\tau_{z\varphi} = \tau_{\max} \left( \frac{r}{r_0} \right)^{\lambda_3-1} \left( 1 - \frac{r-r_0}{R} \right). \quad (3)$$

Eqs. (1a-b) are general and match in some particular cases some well known results of fracture and notch mechanics reported in the literature [8].

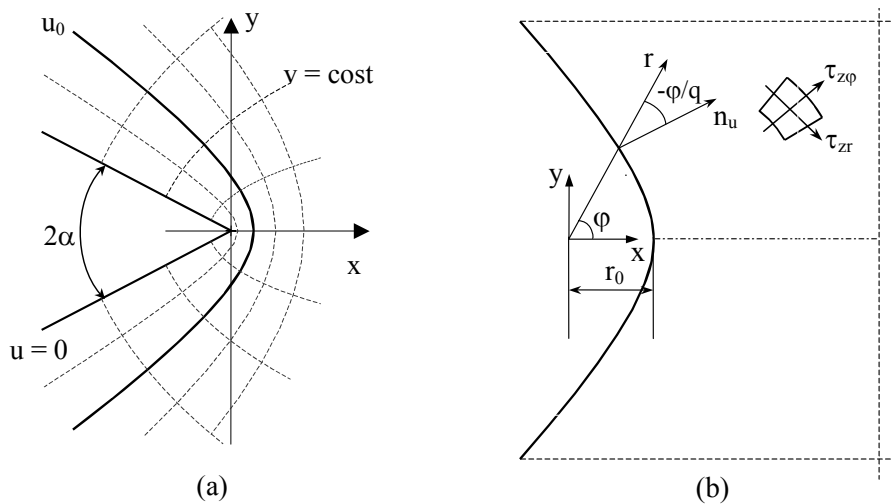


**Fig. 1.** Neuber's system of curvilinear coordinates (u, v) (a); reference system used in the analytical solution (b).

## U- AND V-SHAPED NOTCHES

### *Stress distribution along the notch bisector line for the highly stressed zones*

Due to the very simple form of Eqs. (1, 3) and to the close similarity characterising a circular notch with rectilinear flanks and a hyperbolic notch, it is natural to apply them to both notches, without any clear distinction.

However stress distributions due to operating torsion loadings are very sensible to the notch shape, and geometrical differences in the notch profile may cause a deviation in the flow of stresses within the body, even very close to the notch tip [7].

In particular, the analytical solution obtained in Ref. [8] is able to guarantee the necessary notch free-edge condition only when the notch profile is actually hyperbolic or sharp V- shaped, but generates some residual non-zero shear stresses on the edge in the case of a blunt V- or U-notch; in these cases the prescribed boundary condition on the edge is actually satisfied only at the notch tip, where  $\varphi=0$ , or, approximately, far

from the tip, where  $\varphi \rightarrow \pi - \alpha$ , as shown in figure 2.

For this reason Eqs. (1, 3) when applied to circular-root-notches with rectilinear flanks are approximated, and the degree of accuracy depends both on the notch opening angle and on the notch root radius, ranging between 2% up to 12% (see figure 3). This means that in all the cases where the accuracy of stress distribution is basic Eqs. (1a-b) cannot be applied as they are.

However, an intense numerical study of the problem has highlighted that stresses along the notch bisector line can again be written as a function of a single powered term in the following form [15]:

$$\tau_{z\varphi} = \tau_{\max} \left( \frac{r}{r_0} \right)^{-s_3} \left( 1 - \frac{r - r_0}{R} \right) \quad (5)$$

The exponent  $s_3$  in general is greater than  $(1 - \lambda_3)$ , valid for the corresponding hyperbolic notch; this fact has been thought of as due to the influence of the rectilinear flanks on stress flow, exerting a sort of *closure effect* with respect to the hyperbolic notch with the same opening angle (see also figure 2) [15].

The values of the exponent  $s_3$ , as obtained from a large bulk of numerical results, are listed Table 1, where the notch acuity  $\zeta = a/\rho$  ranges from 2 up to 100. In principle, the more the notch acuity increases, the more the exponent  $s_3$  is expected to deviate from the theoretical value  $(1 - \lambda_3)$ , since the number of discrete points where the previous analytical solution does not satisfy the prescribed boundary condition on the edge increases [15].

However it has been found that when the notch opening angle is equal to or greater than  $90^\circ$ , the influence of the notch acuity on  $s_3$  is so weak to be considered negligible, so that the exponent of stress fields can be thought of as dependent only on the notch opening angle.

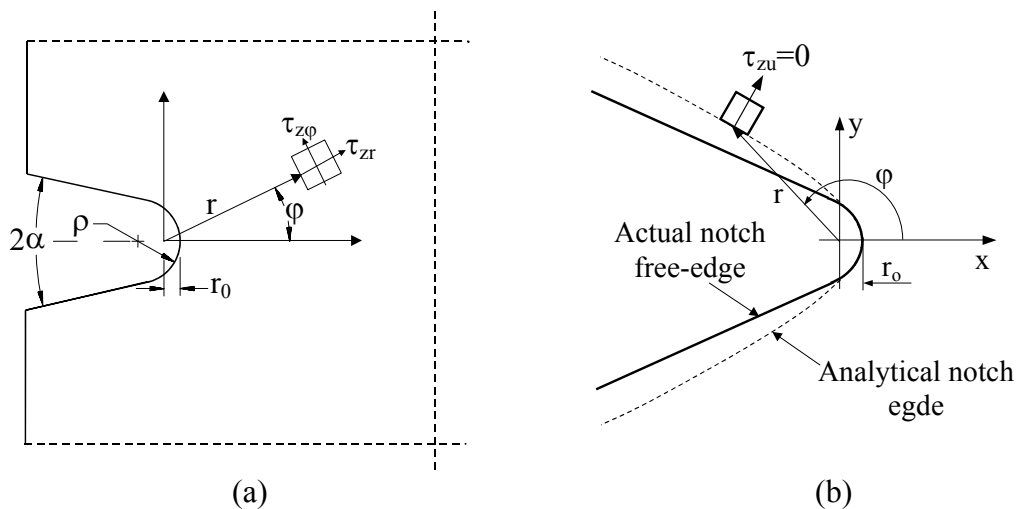


**Fig. 2.** Reference system for a U or rounded V-shape notch (a); geometrical differences existing between a hyperbolic notch and rounded V-shape notch (b).

**Table 1.** Values for coefficient  $s_3$  in Eq. (5)

$2\alpha$ [°]	$s_3$	$2\alpha$ [°]	$s_3$
0	$\frac{17}{30} - \frac{1}{36} \left(\frac{55}{57}\right)^\zeta - \frac{2}{41} \left(\frac{73}{62}\right)^{-\zeta}$	90	0.385
30	$\frac{13}{25} - \frac{1}{23} \left(\frac{57}{74}\right)^\zeta - \frac{1}{38} \left(\frac{22}{21}\right)^{-\zeta}$	120	0.290
60	$\frac{31}{67} - \frac{4}{75} \left(\frac{41}{79}\right)^\zeta - \frac{1}{74} \left(\frac{24}{23}\right)^{-\zeta}$	135	0.235

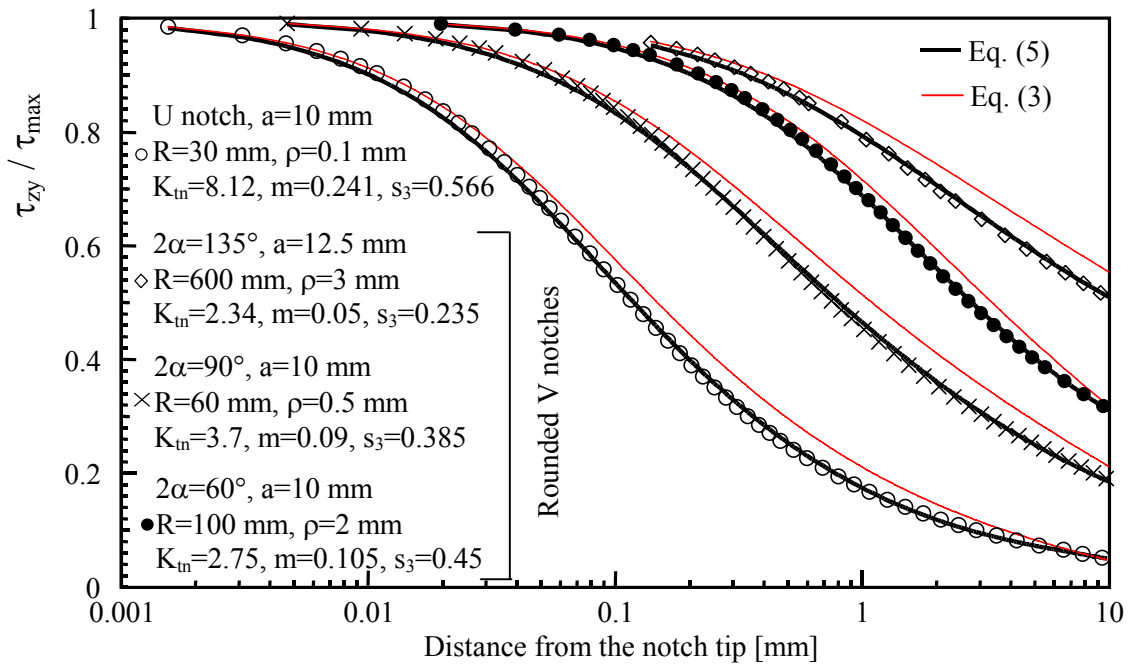


**Figure 3.** Plot of the stress component  $\tau_{zy}$  along the notch bisector line of U- and V-notches in a rounded bar and comparison with Eqs. (3) and (5).

Figure 3 shows a comparison between FE results and Eqs. (3) and (5). It is evident that the proposed correction for stress fields eliminates the inaccuracy previously shown by Eq. (3).

**Evaluation of stresses on the entire ligament**

Due to their nature Eqs. (3, 5) are valid only in the highly-stressed zone close to the notch tip, and not in the nominal zones, where the influence of the notch can be neglected. However, the range of applicability of the solution can be largely extended by substituting the variable  $r$  with the following function:

$$f(r) = r_0 + \frac{\text{Arc tan}[(r - r_0)m]}{m} \tag{6}$$

This function has been already proposed in Refs [12-14] for uniaxially loaded notched components of finite size.

By inserting  $f(r)$  according to Eq. (6) into Eq. (5) one obtains:

$$\tau_{zy}(r,0) = \tau_{\max} \left( 1 + \frac{\text{Arctan}[(r - r_0)m]}{mr_0} \right)^{-s_3} \left( 1 - \frac{r - r_0}{R} \right) \tag{7}$$

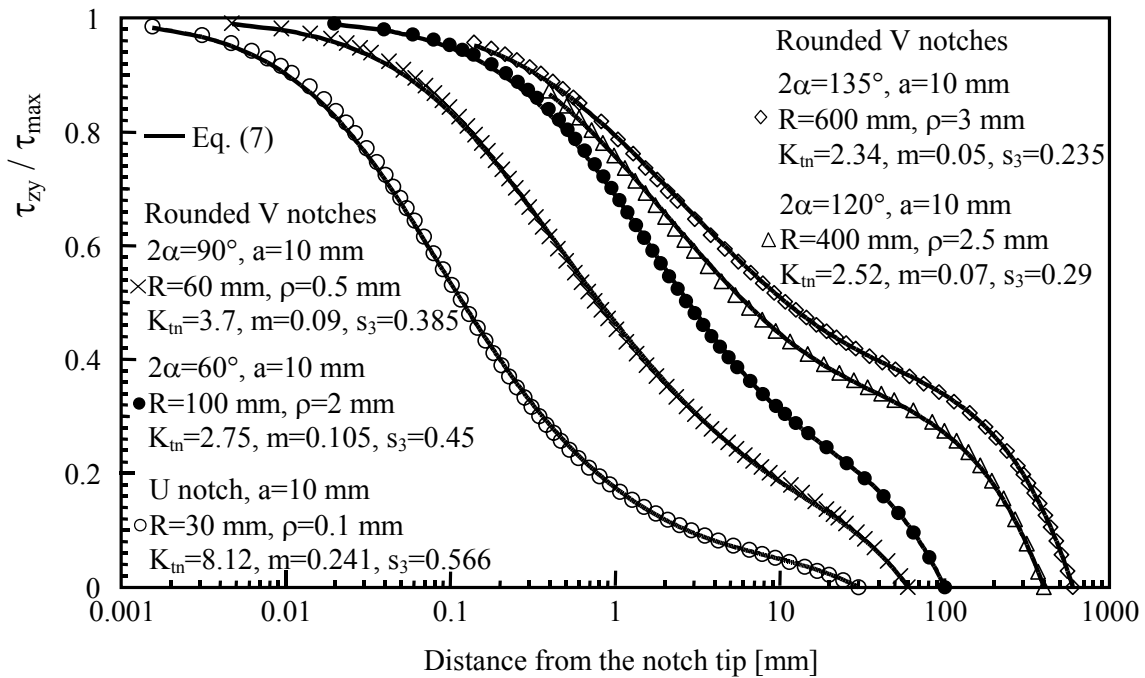


**Figure 4.** Plot of the stress component  $\tau_{zy}$  along the notch bisector line of U- and V-notches in a rounded bar and comparison with Eq. (7).

The value of  $m$  to be used in Eq. (7) can be easily determined by means of a simple equilibrium equation on the net section:

$$\int_0^R \left( 1 + \frac{\text{Arctan}[(R-t)m]}{mr_0} \right)^{-s_3} t^3 dt = \frac{R^4}{4K_{tn}} \quad (8)$$

where the change of variable  $t = R - (r - r_0)$  is used. Here  $K_{tn}$  is the theoretical stress concentration factor referred to the net section of the rounded bar. Eqs. (7, 8) hold valid also for parabolic or hyperbolic notches as soon as  $s_3$  is substituted with  $1 - \lambda_3$ .

Figures 4-6 show a comparison between theoretical predictions and FE results from rounded bars weakened by U- and V-notches. Different opening angles, notch root radius, and ligament widths are considered. It is evident that the agreement is very good for all cases.

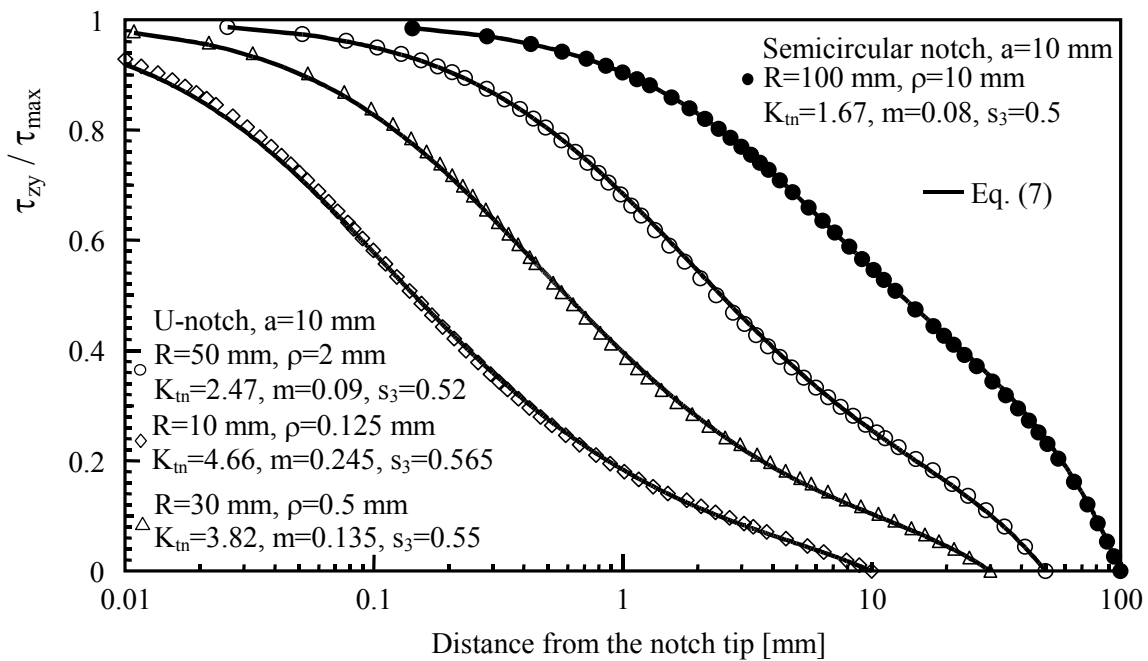


**Figure 5.** Plot of the stress component  $\tau_{zy}$  along the notch bisector line of U- and V-notches in a rounded bar and comparison with Eq. (7).

## CONCLUSIONS

Some new useful expressions for stress distributions induced by U- and V-shaped notches in rounded bars under torsion have been presented.

A simple global equilibrium conditions has been introduce to account for the finite size effect; in this way the shear stress distributions can be accurately determined on the entire net section of the shaft, and not only in the vicinity of the notch tip.

The accuracy of the new relationships is checked by a number of FE analyses carried out on finite size components subjected to torsion loads.

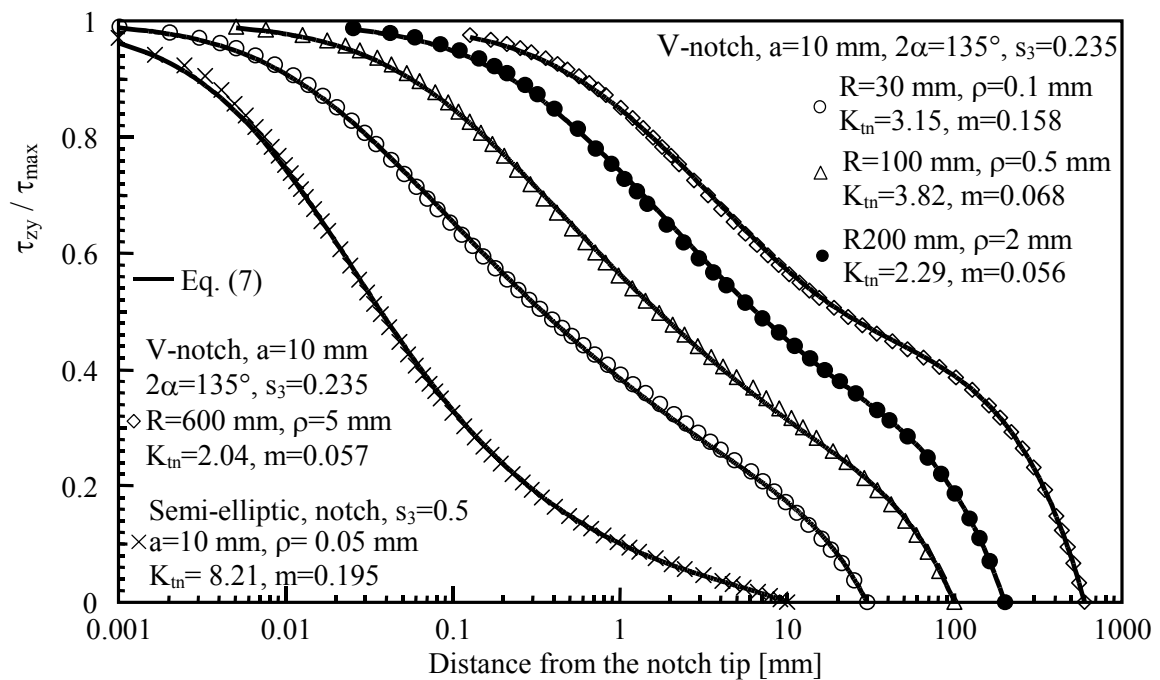


**Figure 6.** Plot of the stress component  $\tau_{zy}$  along the notch bisector line of U- and V-notches in a rounded bar and comparison with Eq. (7).

## REFERENCES

1. Inglis, C.E. (1913) *Trans. Inst. Naval Architects* **55**, 219-30.
2. Westergaard, H.M. (1939) *J. Appl. Mech.* **6**, A49-53.
3. Williams, M. L. (1952) *J. Appl. Mech.* **19**, 526-528.
4. Glinka, G., Newport, A. (1987) *Int. J. Fatigue* **9**, 143-150.
5. Xu, R.X., Thompson, J.C., Topper, T.H. (1995) *Fatigue Fract. Engng. Mater. Struct.* **18**, 885-895.
6. Neuber, H. (1958) *Theory of notch stresses*, Springer-Verlag, Berlin.
7. Lazzarin, P., Zappalorto, M., Yates, J.R. (2007) *Int. J. Eng. Sci.* **45**, (2-8), 308-328.
8. Zappalorto, M., Lazzarin, P., Yates, J.R. (2008) *Int J Solids Struct.* **45**, 4879-4901.
9. Howland, R.J. (1930) *Philos. Trans. R. Soc. Lond. Series A* **229**, 49-86.
10. Ling, C.B. (1947) *J. Appl. Mech.* **14**, A-275-280.
11. Seika, M. (1960) *Ing. Arch.* **27**, 285-294.
12. Atzori, B., Filippi, S., Lazzarin, P. (2003). *Proc. Crack Path 2003*, Parma, Italy.
13. Filippi, S., Lazzarin, P. (2004) *Int. J. Fatigue* **26**, 377-391
14. Atzori, B., Filippi, S., Lazzarin, P., Berto, F. (2005) *Fatigue Fract Engng Mater. Struct.* **28**, 13-2.
15. Zappalorto, M., Filippi, S., Lazzarin, P. Shear stress distributions due to U- and V-notches in finite size rounded bars under torsion, to be submitted.